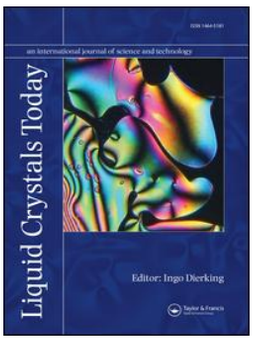

Liquid Crystals Today

ISSN: 1358-314X (Print) 1464-5181 (Online) Journal homepage: https://www.tandfonline.com/loi/tlcy20

The topology of knots and links in nematics

Thomas Machon

To cite this article: Thomas Machon (2019) The topology of knots and links in nematics, Liquid Crystals Today, 28:3, 58-67, DOI: 10.1080/1358314X.2019.1681113

To link to this article: https://doi.org/10.1080/1358314X.2019.1681113

Published online: 02 Dec 2019.

LIQUID CRYSTALS TODAY
2019, VOL. 28, NO. 3, 58–67
https://doi.org/10.1080/1358314X.2019.1681113

Taylor & Francis
Taylor & Francis Group

RESEARCH ARTICLE

OPEN ACCESS Check for updates

The topology of knots and links in nematics

Thomas Machon[a]

[a]H.H. Wills Physics Laboratory, Tyndall Avenue, United Kingdom

ABSTRACT
We review some our results concerning the topology of knotted and linked defects in nematic liquid crystals. We discuss the global topological classification of nematic textures with defects, showing how knotted and linked defect lines have a finite number of 'internal states', counted by the Alexander polynomial of the knot or link. We then give interpretations of these states in terms of umbilic lines, which we also introduce, as well as planar textures. We show how Milnor polynomials can be used to give explicit constructions of these textures. Finally, we discuss some open problems raised by this work.

KEYWORDS
Defects; topology; knots

1 Introduction

In London's Tate Modern, for a long time, there was a piece titled Liquid Crystal Environment by Gustav Metzger[1]. Liquid crystal between two slides, was projected onto the gallery wall, highlighting the thermochromic properties. While beautiful, it always seemed a little sad that a relatively mundane aspect of liquid crystal physics was given such prominence when there is so much intricacy and beauty to be found elsewhere. A more representative piece is the 1978 film 'Transition de Phase dans les Cristaux Liquides' by Jean Painlevé and his childhood friend Yves Bouligand, where we see the some of the true splendour of liquid crystals. More than superficially attractive, the visual beauty of these materials is accompanied by elegance and depth in their theoretical characterisation which, at its heart, often draws on sophisticated geometry and topology. Some of the most interesting examples include the intricate blue phases, with their network of intertwined disclination lines [1]; oily streaks, with their defect crossing rules following Hamilton's quaternionic multiplication [2] and twist-grain boundary phases in smectics [3], analogous to Abrikosov vortex lattices in type-II superconductors, with their connections to Sherck's minimal surfaces [4]. These examples are all from more complex liquid crystalline phases: cholesterics and smectics. In this article, we will focus on topology in the simpler nematics, like the one Metzger shone on the Tate wall.

What we will describe are the abstract topological properties of defects, particularly those which are knotted or linked, but in our mind we have applications to, and descriptions of, experimental work where defect loops are generated in a controlled fashion. Many of these are based on the famous 'Saturn's ring' configuration [5], a defect loop line stabilised around a colloidal particle with homeotropic anchoring conditions [6]. Building on this motif, the Ljubljana group managed to create defect lines entangled around colloidal dimers and wires [7] eventually extending this, in a controlled fashion, to create stabilised knotted defect lines around arrays of colloidal particles [8–10], which experience an attractive interaction when immersed in a liquid crystal. These particles can also be dressed by Skyrmion-like excitations that modify and augment the topology [11]. Further work creating stable disclination loops used higher-genus colloids [12–14], knotted colloids [15], linked particle [16] or colloids simulating non-orientable surfaces [17] to generate stable defect loops. Other work generated controlled arrays of defect loops entangled with a punctured plane [18], generated colloidal particles that themselves simulate a defect line [14] or explored knotted colloids in topological environments [19].

While the experimental systems this work is inspired by are often chiral – many of the structures would not be stable otherwise – this chirality is weak, and the topology of the configurations can be understood by considering the system as a nematic. The historical approach to nematic topology, which we will discuss below first, looks only at the local profile of defect lines. If defect lines become loops, then such a local description becomes inadequate and one needs to consider the entire defect line. An initial examination of this was given in the 80s by Jänich, which we further summarise below; it turns out, however, that Jänich did not find everything, there are additional topological invariants. We will discuss these invariants and give explicit examples of director fields realising them. Then, we will show

CONTACT Thomas Machon t.machon@bristol.ac.uk

how they manifest themselves via the appearance of umbilic lines in the nematic texture, as well as through the quite mysterious notion of 'planar textures'. Finally, we will discuss several open questions in the topology of liquid crystalline defect loops.

It should be pointed out that there is another sense, besides defects, in which knots and links can occur in nematic and cholesteric liquid crystals, which is through the Hopf invariant [20–22]. The knots that appear in this case are not singular, but rather can be seen by looking at the linking of 'pre-images', curves in space where the director field is constant.

2 The basics of topology in nematics

In this article, nematics will be described by a director field **n**, a unit magnitude line field. Because **n** is a line field not a vector field, **n** is equivalent to $-\mathbf{n}$. Because of this, **n** specifies a point on the unit sphere only up to antipodal equivalence, one cannot tell if **n** is pointing up or down. Mathematically, this means that **n** specifies a point not on the unit sphere, S^2, but on the real projective plane $\mathbb{RP}^2$, which can be defined as S^2 with antipodal points identified. Thus, the director field defines a map from the material domain Ω into $\mathbb{RP}^2$. The singularities in this map correspond to the topological defects in the system. The goal of defect classification is to work out how many different types of singularity there are, up to smooth (or continuous) deformation of the configuration.

In two dimensions, nematic point defects have a half-integer charge, as established by Frank [23]. In three dimensions nematic defects are more complex, and can be both points and lines. Their classification is also more subtle, the profiles of all line defects are equivalent (see, e.g. Ref. [24] for an illustration of the $+1/2$ to $-1/2$ transition), the point defects have integer charge, but defects with charges $+q$ and $-q$ are equivalent, a consequence of the $\mathbf{n} \sim -\mathbf{n}$ ambiguity.

To avoid 'forever drawing pictures to convince anyone' that these facts are true [25], modern presentations of the subject rely on the formal mathematics of homotopy theory, as summarised in the classic review by Mermin [26], with a more recent perspective given by Alexander at al [27]. The application of these ideas to nematic defects was originally developed by Kléman and Toulouse [28,29] (who were introduced to the machinery of algebraic topology by Poénaru [30]), and are now central to any serious discussion of defects in liquid crystals, as well as everything we will say below.

As a crude summary[2], the idea of the homotopy theory of defects is to look at the nematic texture on a measuring set around the defect. In the case of a line defect, this measuring set is a circle surrounding the defect line, for a point defect it is the surface of a sphere enclosing the point defect. One then studies the equivalence classes of director fields on these sets up to continuous deformation. This situation is summarised in Figure 1. Because the measuring sets in these two cases are a circle and sphere respectively, it turns out that the topological classes of texture can be given the algebraic structure of a group, which allows you to define addition of defects. This is fairly simple in the case of point defects, but has interesting consequences for defect line crossing in more complex systems (such as biaxial nematics) [31]. In the case of line defects, the group describing the defect classification is given by $\pi_1(\mathbb{RP}^2) \cong \mathbb{Z}_2$, telling us that there are two topological classes of line defect profile, since there are two elements of $\mathbb{Z}_2$. One of these elements is trivial, corresponding to no defect at all, so the homotopy theory tells us that there is only a single topological class of disclination profile in a nematic – as we established earlier. For point defects we look at the second homotopy group of the groundstate manifold $\mathbb{RP}^2$, finding $\pi_2(\mathbb{RP}^2) \cong \mathbb{Z}$. Accounting for the $\mathbf{n} \to -\mathbf{n}$ symmetry reduces this to $\mathbb{N}$ telling us that point defects in 3d nematics are classified by non-negative integers. This reduction of classification from $\mathbb{Z}$ to $\mathbb{N}$ can be subtle. The important point is that for a given texture the $\mathbf{n} \to -\mathbf{n}$ equivalence must be applied globally, see Ref. [27] for an extensive discussion of this issue.

3 Jänich's result

The classic homotopy theory is elegant, but cannot capture the full topological information in a nematic texture. While it works for point defects, it only considers the local

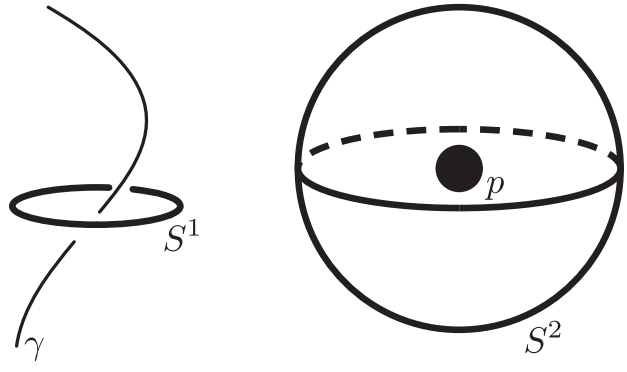

Figure 1. Measuring defect topology in homotopy theory. A line defect, γ is surrounded by a circle, S^1 and a point defect, p is surrounded by a sphere, S^2. In each case, the topology of the defect is determined by studying the restriction of the director **n** to the circle or sphere, resulting in a map $S^n \to \mathbb{RP}^2$.

profile of line defects. If a line defect is in fact a loop, then there is additional global information concerning how the profile connects back to itself (see, for example, the fractional self-linking numbers defined for $-1/2$ profiles defined by Čopar and Žumer [32,33]). Moreover, if the defect lines are knotted or linked then there is additional topological information stored in the nematic texture [34].

While these issues may seem abstract, they become relevant given the plethora of modern experiments, summarised above, in which defect lines can be generated in a controlled fashion. Perhaps (or perhaps not) anticipating such experiments, the first steps in this direction were taken in the 80s by the mathematician Klaus Jänich, in the paper 'Topological properties of ordinary nematics in 3-space' [35]. In this paper, rather than the local profile of a defect line, Jänich considered a toroidal neighbourhood of a defect loop, thus answering the first question of how the local profile of the defect line can connect back on itself. On a toroidal neighbourhood of a defect loop, T^2, the director field defines a map

$$f = u^p + (-iw)^q \tag{1}$$

Jänich then performed a homotopy theoretic calculation, he looked at topological classes of maps from T^2 into $\mathbb{RP}^2$. This gives the topological classes of nematic texture on a torus[3], or equivalently near a defect loop. Jänich showed that these textures are classified by an index v that can take four values, $v \in \{0, 1, 2, 3\}$.

Jänich's index is really in two parts, one of which is simple and the other which is more subtle. First, one should think about the structure of a torus. A torus has two independent non-contractible loops, the longitude and the meridian. If the torus is surrounding a disclination line, then **n** must be non-orientable along the meridian, since this is the topological signature of a disclination, but there is no requirement on the longitude, and **n** can be either orientable or non-orientable along the longitude. This translates as either an even or odd number of disclination loops linking our loop. If there is an even number of loops linking, then $v = 0$ or 2. If there is an odd number then $v = 1$ or 3. This takes care of half the distinct configurations. The remaining freedom is more subtle, while it can be thought of as related to the hedgehog charge of the defect loop [27], this is not the complete story.

First, let us look at the case $v = 0$ or 2. In this case, there is an even number s of other defect lines linking our defect loop. Let us suppose $s = 0$, so that there are no defect lines linking our loop. Then, we can surround the defect loop with a sphere, and measure its hedgehog charge q. There must be some relation between q and v, and in fact if q is even, then $v = 0$ and if q is odd, then $v = 2$. What about the cases $v = 1$ or 3? Well now we cannot play the same trick, because if we try and surround our defect loop with a measuring sphere, we cannot avoid the other defect lines piercing it, making it impossible to measure the hedgehog charge. How then can we interpret this invariant? As we will see below, this invariant can be interpreted as determining the sign of the linking number of the defect lines.

Finally, we note that in addition to providing a classification of defect neighbourhoods, Jänich also provided a topological conservation law for the total set of defects in the system (points and lines) in terms of their local behaviour, though it is not particularly strong, giving only an even/odd conservation.

4 Global classification

While Jänich's result represents a more sophisticated characterisation of defect topology than the basic homotopy theory, it still misses a lot of information. It is fairly easy to see that this must be the case. Consider a system with a single isolated, unknotted, defect loop. By Jänich's classification, the loop must have a particular value of $v \in \{0, 1, 2, 3\}$. Actually, because there is only a single defect loop, it is not linked with any others, so either $v = 0$ or $v = 2$, depending on whether q is even or odd. But we can surround the loop with a sphere, do a topological measurement of the charge, and get an integer $q \in \mathbb{N}_0$. But since this q can take any value, clearly v does not record the entire topology of the configuration. So, a natural question is: can we go further and incorporate all the topological information about the system in our study? The answer to that is yes, and in doing so we reveal new topological information about nematic textures [34,36,37] and in many ways the idea can be thought of as a natural extension of Jänich's work.

In this approach, we throw out no information. This means we study the topology of the entire texture, thought of as a map

$$u^p + (-iw)^q \tag{2}$$

where Ω is the material domain and $\mathcal{D}$ is the defect set. To give a flavour, we will briefly summarise the classification result. To understand the topology of these maps, we need to understand the topology of the space $\Omega \backslash \mathcal{D}$. Ω is a three-dimensional space with zero- and one-dimensional holes in it, which are the defects. Because of this, it is homotopy equivalent to a 2-complex, a space built out of zero-, one- and two-dimensional pieces. It

turns out that the topological classes of these maps are classified by a twisted cohomology group, which we write as

$$H^2(\Omega\backslash\mathcal{D};\mathbb{Z}^\omega) \tag{3}$$

where $\mathbb{Z}^\omega$ is a coefficient system which encodes the $\mathbf{n} \to -\mathbf{n}$ transformation associated with disclination lines. The classification is given by this group along with the equivalence relation $x \sim -x$, where x is a group element.

This result is a complete classification of defect topology, subsuming the classical homotopy theoretic approach, as well as Jänich's result. As written, however, it is extremely opaque. It becomes a little clearer when we evaluate it for specific cases. First, let us consider the simple case when we have N point defects and no line defects. In this case, we can write

$$H^2(\Omega\backslash\mathcal{D};\mathbb{Z}^\omega) = \mathbb{Z}^N. \tag{4}$$

What this means is that we get to choose an integer charge for each point defect – we recover the standard homotopy theoretic result. Accounting for the equivalence relation means we identify configurations $(q_1, q_2, \ldots, q_N)$, with $-(q_1, q_2, \ldots, q_N)$, where q_i is the charge of the i^{th} point defect, the $\mathbf{n} \to -\mathbf{n}$ symmetry must be applied globally.

Now let's think about a single defect loop. Suppose further that it is a knot, K, then it turns out that we can write

$$H^2(\Omega\backslash K;\mathbb{Z}^\omega) = \mathbb{Z} \oplus G(K) \tag{5}$$

Now the classification has two pieces, the integer factor $\mathbb{Z}$ and the additional piece $G(K)$. The integer factor is the same as before, it simply encodes the hedgehog charge of the defect loop, as measured by a sphere surrounding it. The interesting piece is the second part, $G(K)$. This is a finite group (at least for a knot) which depends only on the knot type. For example, if we have an unknot $G(K) = 1$, the trivial group. If K is a trefoil knot then $G(K) = \mathbb{Z}_3$, the cyclic group of order 3. For a knot, $G(K)$ is always a finite group of odd order, given by the Alexander polynomial evaluated at -1, neither of these facts are true if K is a link (having multiple components). Let us take the example of the trefoil knot, where $G(K) = \mathbb{Z}_3$. This means there are three distinct topological classes of nematic texture surrounding a trefoil knot defect. We will discuss their physical interpretation later.

Now let's think about a general collection of defects. It turns out that from the perspective of nematic topology, the natural way to think about them is in terms of split components. This means that we have the set of defects, $\mathcal{D}$ decomposed as a set of point defects, $\mathcal{P}$, and a set of line defects, $\mathcal{L}$ which we decompose into collections of defects that can be surrounded by a sphere (split components), as illustrated in Figure 2. Note that each split component may contain more than one line defect. We can then write

$$H^2(\Omega\backslash\mathcal{D};\mathbb{Z}^\omega) = \left(\bigoplus_{p_i\in\mathcal{P}} \mathbb{Z}\right) \oplus \left(\bigoplus_{L_j\in\mathcal{L}} (\mathbb{Z} \oplus G(L_j))\right)/x \sim -x. \tag{6}$$

This formula has a simple interpretation. The global classification assigns an integer charge to each point defect, and to each split component of the set of line defects there is also the integer charge, as well as an element of the group $G(K)$. From a topological perspective one can think of each split component as a 'particle', with a charge as well as an internal state, the internal state being given by an element of the group $G(K)$, as illustrated in Figure 2. This internal state describes the topologically distinct nematic textures in the complement of the knot or link. We note that for complex arrangements of defects $G(K)$ can

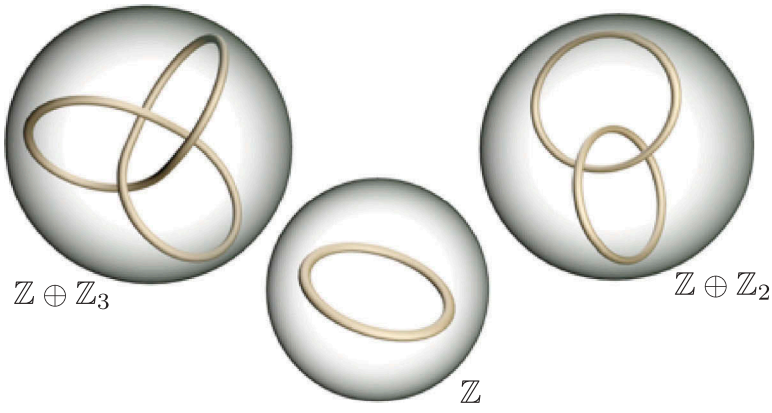

Figure 2. Split components of line defects, here there are three: an unknot, a trefoil knot and a Hopf link. The topological classification of textures with this defect set is given by an integer charge for each split component, a $\mathbb{Z}_3$ internal state for the trefoil knot and a $\mathbb{Z}_2$ internal state for the Hopf link, along with a global $x \sim -x$ relation corresponding to the $\mathbf{n} \sim -\mathbf{n}$ symmetry of the nematic.

have very interesting properties. For example in Ref. [38] an array of woven defect lines is considered where we find a correspondence between topological classes of nematic configurations and recurrent stable states in the Abelian sandpile model of statistical mechanics.

5 Interpretations: umbilines and planar textures

In our classification result [6] the integer factors are well understood and familiar: they correspond to point defect charges. The internal states, however, are not so familiar, and so must be understood in a different way. In fact, not all internal states have the same interpretation. Here we will give two ways in which they are distinct from each other – by the mandated existence of umbilic lines (or Skyrmion tubes) as well as the existence of more mysterious 'planar textures', which we associate to linking numbers of defect lines.

Let us first introduce the idea of umbilic lines [39]. These originate in the decomposition of the gradient tensor $\nabla\mathbf{n}$ [40]. Suppose $\mathbf{n}$ is equal to $(0,0,1)$ at some point, then at that point we can write the gradient tensor $\nabla\mathbf{n}$ as

$$\nabla\mathbf{n} = \frac{\nabla\cdot\mathbf{n}}{2}\begin{pmatrix}1&0&0\\0&1&0\\0&0&0\end{pmatrix} + \frac{\mathbf{n}\cdot\nabla\times\mathbf{n}}{2}\begin{pmatrix}0&-1&0\\1&0&0\\0&0&0\end{pmatrix} + n_i b_j + \Delta \tag{7}$$

where $b = (\mathbf{n}\cdot\nabla)\mathbf{n} = -\mathbf{n}\times\nabla\times\mathbf{n}$ is the bend vector. The extra piece Δ can be written as

$$\Delta = \frac{1}{2}\begin{pmatrix}\partial_1 n_1 - \partial_2 n_2 & \partial_1 n_2 + \partial_2 n_1 & 0\\ \partial_1 n_2 + \partial_2 n_1 & \partial_2 n_2 - \partial_2 n_1 & 0\\ 0 & 0 & 0\end{pmatrix} \tag{8}$$

and is a traceless symmetric tensor orthogonal to $\mathbf{n}$, so that $n_i\Delta_{ij} = 0_j$. Writing the gradient tensor this way is the first step to deriving the Frank free energy, this decomposition respects rotations of the coordinate system that preserve the director field. Correspondingly, the squared magnitude of each piece is a symmetry protected scalar. We can readily identify splay, twist and bend as the first three pieces. The last piece, Δ, must therefore correspond to saddle-splay. This is true, but it is not the whole story, taking the magnitude of Δ we find

$$|\Delta|^2 = \Delta_{ij}\Delta_{ij} = \mathrm{Tr}\Delta^2 = \left(\frac{\nabla\cdot\mathbf{n}}{2}\right)^2 + \left(\frac{\mathbf{n}\cdot\nabla\times\mathbf{n}}{2}\right)^2 - \frac{1}{2}\nabla\cdot(\mathbf{n}(\nabla\cdot\mathbf{n}) - (\mathbf{n}\cdot\nabla)\mathbf{n}) \geq 0 \tag{9}$$

where the quantity on the second line is the familiar saddle-splay. So while saddle-splay is part of $|\Delta^2|$ it is not the entirety and indeed saddle-splay can only be negative if splay and twist are sufficiently high that the inequality is satisfied.

Splay, twist and bend all have fairly well-defined geometric meanings. Splay measures the degree to which a flow along $\mathbf{n}$ preserves volume – i.e. how much $\mathbf{n}$ is spreading things out. Twist is a pseudoscalar measuring the chirality of the director field and if it vanishes, then $\mathbf{n}$ is the normal vector to a family of surfaces. Bend simply gives the curvature of integral curves of the director field. What about $|\Delta|^2$? It is not equal to saddle-splay. To understand Δ, you must understand what it is not. The tensors associated to splay and twist are isotropic in directions orthogonal to $\mathbf{n}$, being the identity matrix and Levi-Civita tensor in the *xy* plane, respectively. The bend vector characterises the gradients *along* $\mathbf{n}$, so all that is left are the anisotropic orthogonal gradients of $\mathbf{n}$ – these are characterised by Δ. We point out that the phrase 'anisotropic orthogonal gradients of $\mathbf{n}$' was recently deemed 'too long for common use' [40] and repeat it here with pleasure.

Now let's consider places where $|\Delta|^2 = 0$. Δ has two independent components, $\partial_1 n_1 - \partial_2 n_2$ and $\partial_1 n_2 + \partial_2 n_1$, and for $|\Delta|^2 = 0$ they both must vanish. This means that zeros of Δ occur along lines in space. In Ref. [39], we called these umbilic lines because if the twist vanishes, then the zeros of Δ are the lines of umbilic points of the surfaces whose normal is $\mathbf{n}$. These lines are then regions where the gradients of $\mathbf{n}$ are isotropic in directions orthogonal to $\mathbf{n}$. This means that they are the cores of vortex structures. In fact, they are the centers of Skyrmions, λ-lines and other structures seen in orientational order. Some of the simplest examples are the axisymmetric structures shown in Figure 3, these have the explicit expression

$$\mathbf{n} = \cos r\mathbf{e}_z + \sin r(\cos t\mathbf{e}_r - \sin t\mathbf{e}_\phi), \tag{10}$$

where (r,ϕ,z) are cylindrical coordinates and t is a parameter with $t = 0$ corresponding to the curvature vortex and $t = \pi/2$ the torsion vortex. A quick computation shows that in these cases, $|\Delta|^2$ has an expansion

$$|\Delta|^2 \approx \frac{1}{72}(5 - 3\cos 2t)r^4 + O(r^6), \tag{11}$$

confirming that at the origin we have an umbilic. Note that $|\Delta|^2$ goes to zero as r^4, rather than the lowest order generic behaviour of r^2. This is because these axisymmetric structures are not the lowest order umbilic lines. The lowest order, or generic, umbilic lines have a half-winding profile, and can be recognised as λ lines in cholesterics, as shown in Figure 4.

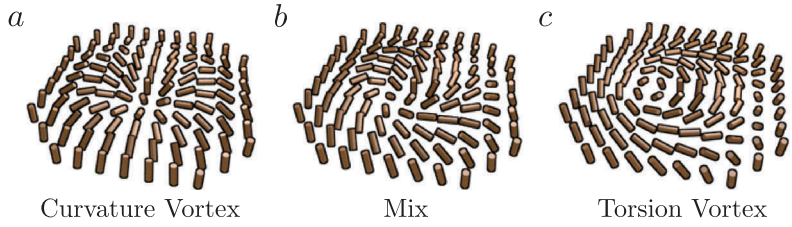

Figure 3. Vortex structures in a director field, commonly seen as Skyrmion distortions, their cores are umbilic lines. They have the explicit expression [10]. These are not the lowest order (generic) umbilic lines, which have a $1/2$ winding, as shown in Figure 4.

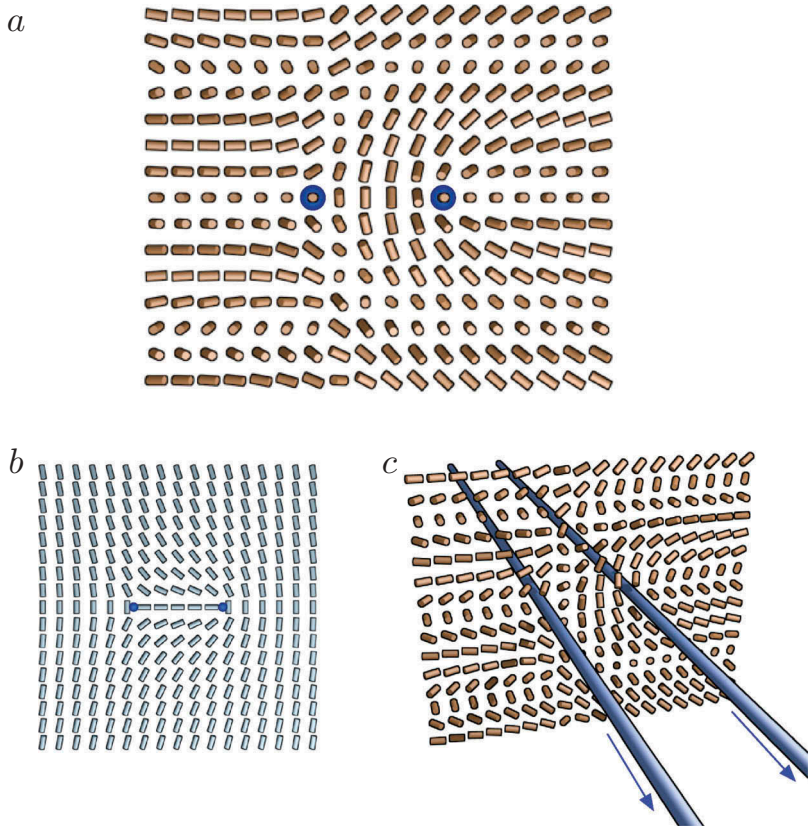

Figure 4. Generic umbilic lines realised as a $\lambda^{\pm}$ pair. (a) Director field $\mathbf{n}$ of the cross-section with umbilics shown in dark blue. (b) Eigenfield of the tensor Δ. As discussed in Ref. [39], these directions may be thought of as the local pitch axis. The singularities are where the eigenvectors are degenerate, which means $|\Delta|^2 = 0$, i.e. we are on an umbilic line. (c) Three-dimensional image illustrating the umbilic lines. The arrows denote the orientation of the umbilic. While we do not discuss this in detail here, it is explained thoroughly in Ref. [39].

What connection do these umbilic lines have to knotted defects? Well, it turns out that the topology of the umbilic lines represents part of the topology of the texture. We will explain this first with reference to a simple case, a Saturn's ring, this is shown in Figure 5. The relationship is essentially a version of the Poincaré-Hopf theorem. Consider the standard Saturn's ring setup, a colloidal particle with homoetropic (normal) anchoring with a stable disclination loop surrounding it and far-field boundary conditions of $\mathbf{n}$ vertical. Figure 5 shows a case with chirality, this breaks the rotational symmetry which otherwise makes the gradients degenerate. The umbilic lines in this system are the zeros of $|\Delta|^2$, or equivalently they are singularities in an eigenvector field of Δ. Now the eigenvectors of Δ must be orthogonal to $\mathbf{n}$, because $\mathbf{n} \cdot \Delta = 0$. This means that close to the colloidal particle the eigenvectors of Δ approximate a director field tangent to the sphere, because of the homeotropic boundary conditions. But the hairy ball theorem (Poincaré-Hopf) says that such a director field must have zeros of total winding $+2 = \chi(S^2)$, hence the eigenvector field must have zeros and we must have umbilic lines coming out of the sphere. Where do they end? the umbilic lines carry

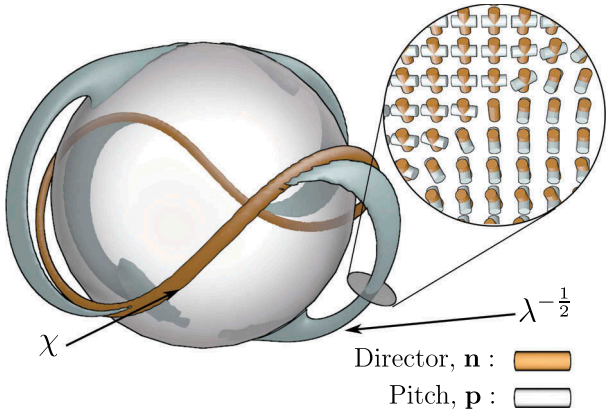

Figure 5. Umbilic lines around a Saturn's ring configuration in a chiral system. The defect line is shown in brown. The four gray lines are umbilic lines and connect the defect line to the colloid. As shown in the inset, the umbilic lines are singularities in the 'pitch', defined here as an eigenvector of the tensor Δ. The total number of umbilic lines, 4, is controlled by [13].

the hedgehog charge, since in the far field there is no hedgehog charge they must end on the disclination loop, as shown in Figure 5.

So we see that umbilic lines carry topological information about the texture, related to hedgehog charge. In fact, in general we have the following result [39]. Suppose $\mathbf{n}$ is a nematic director field. Then, up to sign the topology of $\mathbf{n}$ determines an element of the twisted cohomology group

$$[\mathbf{n}] \in H^2(\Omega; \mathbb{Z}^\omega). \tag{12}$$

Now look at the set of umbilic lines, Γ. Γ, it turns out, defines an element of the Poincaré dual to the twisted cohomology group. It follows that the Poincaré dual (PD) of Γ, of the umbilic lines, must be related to $\mathbf{n}$. In fact we have

$$\mathrm{PD}[\Gamma] = 4[\mathbf{n}]. \tag{13}$$

This means that given $\mathbf{n}$, there are certain topologically mandated umbilic lines that must exist. Alternatively, one can view this as telling you about the distinction between different textures around knotted and linked defect lines – they differ in terms of the number of umbilic lines. Note that in Figure 5 the colloidal particle has charge $+1$ and there are 4 umbilics attached to it, matching [13].

This becomes particularly interesting in the case of knots and links. Because the topological classification has parts which are finite groups, it turns out that sometimes $4[\mathbf{n}] = 0$. For example, in the case of the Hopf link the classification is given by $\mathbb{Z}_2$, i.e. 0 and 1 under addition modulo 2. Well, $4 \times 0 \equiv 0 \mod 2$ and $4 \times 1 \equiv 0 \mod 2$, so neither of the textures associated to the Hopf link have an interpretation in terms of topologically required umbilic lines. On the other hand, if the defect line is a knot, then the classification is by a finite group of odd order. It is easy to show that no element of such a group can ever satisfy $4x = 0$, so all textures around knotted defects have an interpretation in terms of umbilic lines.

So, given that we cannot interpret the textures for which $4[\mathbf{n}] = 0$ in terms of umbilic lines, how should we interpret them? This is a very subtle question, and we do not have a complete answer. Currently, we can say textures for which $2[\mathbf{n}] = 0$ are in some sense 'planar'. Textures for which $4[\mathbf{n}] = 0$ but $2[\mathbf{n}] \neq 0$ are more complex, and we conjecture that they are associated with the existence of τ lines.

Let us address the planar textures first. Consider the case of two linked defect loops. As we have discussed, the topological classification of textures surrounding them is given by an element of the group $\mathbb{Z}_2$. As we will show with explicit examples below, both these textures have the property that they may all be brought into a planar form, by which we mean the director points everywhere in the xy-plane. On the other hand, this is not possible for the texture around a point defect with non-zero charge. This planar/non-planar distinction defines a basic dichotomy in the classification of nematic textures. It turns out [36] that planar textures have a simple characterisation in terms of the twisted cohomology group, corresponding to elements satisfying $2[\mathbf{n}] = 0$. This is a technical result involving the computation of a cohomology group with a coefficient system given by the twisted relative homotopy group $\pi_2(\mathbb{RP}^2, \mathbb{RP}^1)^\omega$ and we refer the reader to Ref. [36] for details.

The interpretation of planar textures is difficult. We know that some of them can be associated to 'linking numbers' of defects [34,36], but in general the full characterisation remains a mystery. So now we have essentially two characterisations of textures. The elements of order 2 correspond to textures that can be brought into planar form. The elements which are not of order 4 can be thought of as being decorated by umbilic lines – or local Skyrmion distortions, this includes point defects, which generally will have $4q$ umbilic lines attached, where q is the charge. The only gap in this description are elements which are of order 4 but not of order 2. In Ref. [36], we suggest that these are associated with textures that can be brought into a form where they contain only χ and τ lines, to borrow the cholesteric classification. However, we have not proved this and it would be interesting to see a more thorough investigation.

6 Examples: the Hopf link and the trefoil knot

It is very helpful, in understanding this classification, to be able to produce explicit examples of textures in a given topological class, surrounding a given defect

set. From the outside, it appears that giving such examples is difficult, one must first write down a nematic director field, and then determine its topology, which can be done using the Pontryagin-Thom construction [20]. To write down explicit examples of knotted fields we use Milnor fibrations [41–44], which have become fairly common in the construction of explicit field configurations containing knots, finding applications also in optics [45] as well as electromagnetism [46,47] for example. The basic idea is to write down a certain polynomial in two complex variables u and w. The canonical examples are the Brieskorn [48] polynomials

$$f(u,w) = u^p - w^q \tag{14}$$

which produce torus knots. To turn this into a nematic texture, one writes the complex variables u and w in terms of Cartesian coordinates, x, y and z, using stereographic projection as

$$(u,w) = \frac{1}{1+r^2}\left(2x + i2y, 2z + i(1-r^2)\right) \tag{15}$$

where $r^2 = x^2 + y^2 + z^2$. This gives a complex valued function $f(x,y,z)$. The zeros of this function are codimension 2, and so lie along lines in space, and it can be verified that in this case the lines are (p,q) torus knots or links. Around these lines the phase of f winds by 2π. The idea is to take the 'square-root' of this polynomial, to get a new function around whose zeros the phase winds by only π, this new phase function will therefore have disclination lines along torus knot components. If φ is the phase of $f(x,y,z)$, then we write down the director field as

$$\mathbf{n} = (\sin\frac{1}{2}\varphi, 0, \cos\frac{1}{2}\varphi) \tag{16}$$

Typically, we would like $\mathbf{n}$ to point in the vertical direction as $r \to \infty$. This can easily be achieved by a phase shift, or equivalently using the normalisation condition for the polynomials $f = u^p + (-i)w^q$. There are several further choices we can make for the textures. The polynomials $u^p + (-i)w^q$ factor into $\gcd(p,q)$ terms, with each term representing a different component of the torus link. For example, the Hopf link with $p = q = 2$ there are two components, and accordingly the polynomial factorises as

$$f(u,w) = (u+w)(u-w), \tag{17}$$

but recall that the zeros of this polynomial determine the structure of the defect set. With this in mind, we can take the conjugate of one of the factors, obtaining the new polynomial

$$f(u,w) = (u+w)\overline{(u-w)}. \tag{18}$$

This new polynomial still has a Hopf link defect, and the phase still winds by 2π around each of the defect lines, but the direction of the winding is reversed for the second component.

Figure 6 shows illustrations of the textures produced by [16] for the two Hopf link polynomials as well as the trefoil knot ($p = 3$, $q = 2$). What is shown is the surface where $\varphi = \pi$, i.e. where $\mathbf{n} = \mathbf{e}_x$, this is a fibre of the Milnor fibration. Note that for the two Hopf links the surfaces are different, and one can associate different linking numbers to the defects by using the right-hand rule to orient the defects. It turns out [34,36] that these two textures correspond to the two distinct internal states of the Hopf link (recall the $\mathbb{Z}_2$) classification.

We have one additional freedom, in our director field [16] we only used the x- and z- orientations, and there is an additional degree of freedom, this can be incorporated by adding a new angle field χ and writing the director field as

$$\mathbf{n} = (\sin\frac{1}{2}\varphi\cos\chi, \sin\frac{1}{2}\varphi\sin\chi, \cos\frac{1}{2}\varphi) \tag{19}$$

χ can be used to modify the topology of the texture, in particular by incorporating singularities. As long as the

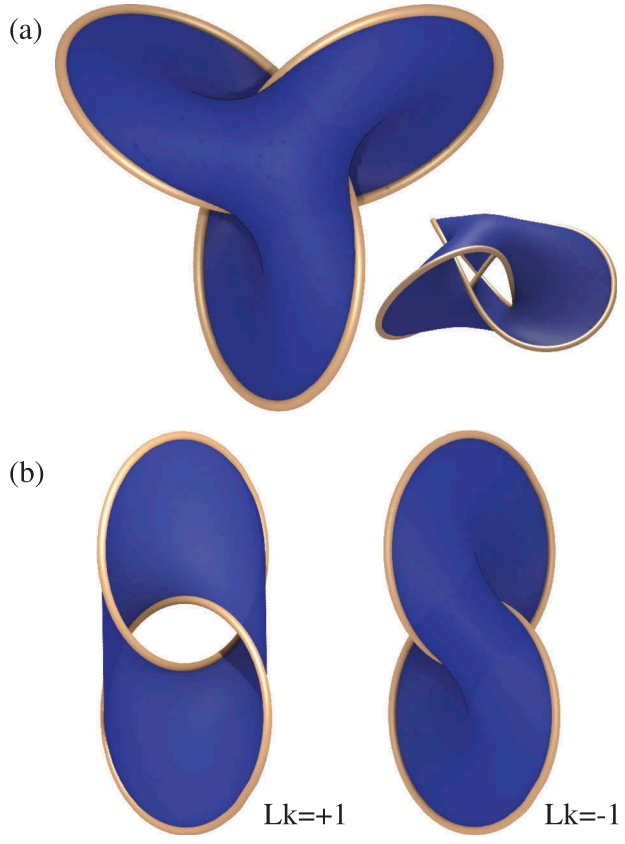

Figure 6. Surfaces where $\mathbf{n} = \mathbf{e}_x$ around Hopf link and trefoil knot textures produced using Milnor polynomials, note the different linking numbers.

singularities in χ do not intersect the surfaces where $\sin\varphi/2 = \pm 1$, then the resulting discontinuities in **n** can be smoothed out [37], to obtain a new director field. The singularities in χ define a set of curves, which can be used to add Skyrmion tubes or umbilic lines to textures.

7 Conclusions and future perspectives

We summarised our recent results on the global topology of nematic liquid crystals, showing that when nematic defects are knotted, a large number of new global topological invariants arise, associated to a twisted cohomology group and counted by the Alexander polynomial of knot theory. We showed how to explicitly construct textures realising these invariants and gave a physical interpretation for them through the use of umbilic lines and the idea of planar textures. Despite this, many questions still remain. For example, what happens when defects cross? The local change in the topology can be understood from Jänich's result, but the global change is much more subtle. In particular, because the knot type changes, the global classification changes, and one must understand how the topological invariants map from one knot to another. In addition, while we have given a crude understanding of planar textures in terms of linking numbers and τ lines, the full picture is still far from complete. Finally, what happens when the system is not just a nematic? For example, in the case of the smectic there are subtle issues to do with whether the knot is fibred, in cholesterics one expects a far greater number of metastable states due to the tendency of the cholesteric to twist. We have proposed contact topology as an appropriate tool with which to study such structures [49], but it remains far from a complete picture.

Notes

1. Tate Reference: T12160.
2. This paragraph runs the risk of being unintelligible to those who are not familiar with these ideas and irrelevant for those who are. However, it is traditional for at least one such paragraph to be included in every scientific article.
3. There is a slight technical difficulty here, because a torus is not an *n*-dimensional sphere, homotopy classes of maps do not have the structure of a group, so the result can be more complicated.

Disclosure statement

No potential conflict of interest was reported by the author.

References

[1] Wright DC, Mermin ND. Crystalline liquids: the blue phases. Rev Mod Phys. 1989;61:385.
[2] Bouligand Y, Derrifa D, Poénaru V, et al. Distortions with double topological character: the case of cholesterics. J Phys France. 1978;39:863.
[3] Renn SR, Lubensky TC. Abrikosov dislocation lattice in a model of the cholesteric–to–smectic-A transition. Phys Rev A. 1988;38(4):2132.
[4] Kamien RD, Lubensky TC. Minimal surfaces, screw dislocations, and twist grain boundaries. Phys Rev Lett. 1999;82:2892.
[5] Terentjev EM. Disclination loops, standing alone and around solid particles, in nematic liquid crystals. Phys Rev E. 1995;51:1330.
[6] Gu Y, Abbott NL. Observation of saturn-ring defects around solid microspheres in nematic liquid crystals. Phys Rev Lett. 2000;85:4719.
[7] Ravnik M, Škarabot M, Žumer S, et al. Entangled nematic colloidal dimers and wires. Phys Rev Lett. 2007;99:247801.
[8] Jampani VSR, Škarabot M, Ravnik M, et al. Colloidal entanglement in highly twisted chiral nematic colloids: twisted loops, Hopf links, and trefoil knots. Phys Rev E. 2011;84:031703.
[9] Tkalec U, Ravnik M, Čopar S, et al. Reconfigurable knots and links in chiral nematic colloids. Science. 2011;33:62.
[10] Čopar S, Tkalec U, Muševič I, et al. Knot theory realizations in nematic colloids. Proc Natl Acad Sci USA. 2015;112:1675.
[11] Pandey MB, Porenta T, Brewer J, et al. Self-assembly of skyrmion-dressed chiral nematic colloids with tangential anchoring. Phys Rev E. 2014;89:060502.
[12] Senyuk B, Liu Q, He S, et al. Topological colloids. Nature. 2013;493:200.
[13] Liu Q, Senyuk B, Tasinkevych M, et al. Nematic liquid crystal boojums with handles on colloidal handlebodies. Proc Natl Acad Sci USA. 2013;110:9231.
[14] Cavallaro M Jr, Gharbi MA, Beller DA, et al. Ring around the colloid. Soft Matter. 2013;9:9099.
[15] Martinez A, Ravnik M, Lucero B, et al. Mutually tangled colloidal knots and induced defect loops in nematic fields. Nat Mater. 2014;13:258.
[16] Martinez A, Hermosillo L, Tasinkevych M, et al. Linked topological colloids in a nematic host. Proc Natl Acad Sci USA. 2015;112:4546.
[17] Machon T, Alexander GP. Knots and nonorientable surfaces in chiral nematics. Proc Natl Acad Sci USA. 2013;110(35):14174–14179.
[18] Tran L, Lavrentovich MO, Beller DA, et al. Lassoing saddle splay and the geometrical control of topological defects. Proc Natl Acad Sci USA. 2016;113:7106.
[19] Hashemi SM, Ravnik M. Nematic colloidal knots in topological environments. Soft Matter. 2018;14:4935.
[20] Chen BG, Ackerman PJ, Alexander GP, et al. Generating the Hopf fibration experimentally in nematic liquid crystals. Phys Rev Lett. 2013;110:237801.
[21] Ackerman PJ, Smalyukh II. Static three-dimensional topological solitons in fluid chiral ferromagnets and colloids. Nat Mater. 2017;16:426.
[22] Ackerman PJ, Smalyukh II. Diversity of Knot Solitons in Liquid Crystals Manifested by Linking of Preimages in Torons and Hopfions. Phys Rev X. 2017;7:011006.

[23] Frank FC. I. Liquid crystals. On the theory of liquid crystals. Discuss Faraday Soc. 1958;25:19–28.
[24] Čopar S, Žumer S. Quaternions and hybrid nematic disclinations. Proc R Soc A. 2013;469:2156.
[25] Sethna JP. Statistical mechanics: entropy, order parameters, and complexity. USA: Oxford University Press; 2006.
[26] Mermin ND. The topological theory of defects in ordered media. Rev Mod Phys. 1979;51:591.
[27] Alexander GP, Chen BG, Matsumoto EA, et al. Colloquium: disclination loops, point defects, and all that in nematic liquid crystals. Rev Mod Phys. 2012;84:497.
[28] Toulouse G, Kléman M. Principles of a classification of defects in ordered media. J Phys Paris. 1976;37:149.
[29] Kléman M, Michel L, Toulouse G. Classification of topologically stable defects in ordered media. J Phys Lett. 1977;38:195.
[30] Kamien RD. Private communication. 2019.
[31] Poénaru V, Toulouse G. The crossing of defects in ordered media and the topology of 3-manifolds. J Physique. 1977;38:887.
[32] Čopar S, Žumer S. Nematic braids: topological invariants and rewiring of disclinations. Phys Rev Lett. 2011;106:117801.
[33] Čopar S. Topology and geometry of nematic braids. Phys Rep. 2014;538:1.
[34] Machon T, Alexander GP. Knotted defects in nematic liquid crystals. Phys Rev Lett. 2014;113:027801.
[35] Jänich K. Topological properties of ordinary nematics in 3-space. Acta Appl Math. 1987;8:65.
[36] Machon T, Alexander GP. Global defect topology in nematic liquid crystals. Proc R Soc A. 2016;472:20160265.
[37] Machon T [PhD Thesis]. University of Warwick; 2016.
[38] Machon T, Alexander GP. Woven nematic defects, skyrmions, and the abelian sandpile model. Phys Rev Lett. 2018;121:237801.
[39] Machon T, Alexander GP. Umbilic lines in orientational order. Phys Rev X. 2016;6:011033.
[40] Selinger JV. Interpretation of saddle-splay and the Oseen-Frank free energy in liquid crystals. Liq. Cryst. Rev. 2018;6(2):129-142.
[41] Milnor JW. Singular points of complex hypersurfaces. Princeton: Princeton University Press; 1968.
[42] Binysh J, Alexander GP. Maxwell's theory of solid angle and the construction of knotted fields. J Phys A Math Theor. 2018;51:385202.
[43] Bode B, Dennis MR, Foster D, et al. Knotted fields and explicit fibrations for lemniscate knots. Proc R Soc A. 2017;473:20160829.
[44] Dennis MR, Bode B. Constructing a polynomial whose nodal set is the three-twist knot. J Phys A Math Theor. 2017;50:265204.
[45] Dennis MR, King RP, Jack B, et al. Isolated optical vortex knots. Nat Phys. 2010;6:118.
[46] Irvine WTM. Linked and knotted beams of light, conservation of helicity and the flow of null electromagnetic fields. J Phys A Math Theor. 2010;43:385203.
[47] Kedia H, Bialynicki-Birula I, Peralta-Salas D, et al. Tying knots in light fields. Phys Rev Lett. 2013;111:150404.
[48] Brieskorn E. Beispiele zur differentialtopologie von singularitäten. Invent Math. 1966;2:1.
[49] Machon T. Contact topology and the structure and dynamics of cholesterics. New J Phys. 2017;19:113030.